POLITECNICO DI TORINO
Repository ISTITUZIONALE

Physics-Based Time-Domain Modeling of VCSELs

*Original*
Physics-Based Time-Domain Modeling of VCSELs / D'Alessandro, Martino; Gullino, Alberto; Tibaldi, Alberto; Bertazzi, Francesco; Goano, Michele; Debernardi, Pierluigi. - ELETTRONICO. - 2022 International Conference on Numerical Simulation of Optoelectronic Devices (NUSOD):(2022), pp. 61-62. (Intervento presentato al convegno 2022 International Conference on Numerical Simulation of Optoelectronic Devices (NUSOD) tenutosi a Torino, Italia nel 12-16 settembre 2022) [10.1109/NUSOD54938.2022.9894787].

*Availability:*
This version is available at: 11583/2971774 since: 2022-09-27T09:35:20Z

*Publisher:*
IEEE

*Published*
DOI:10.1109/NUSOD54938.2022.9894787

*Terms of use:*

This article is made available under terms and conditions as specified in the corresponding bibliographic description in the repository

*Publisher copyright*
IEEE postprint/Author's Accepted Manuscript

©2022 IEEE. Personal use of this material is permitted. Permission from IEEE must be obtained for all other uses, in any current or future media, including reprinting/republishing this material for advertising or promotional purposes, creating new collecting works, for resale or lists, or reuse of any copyrighted component of this work in other works.

(Article begins on next page)

24 April 2024

# Physics-based time-domain modeling of VCSELs

Martino D'Alessandro*, Alberto Gullino*, Alberto Tibaldi*†, Francesco Bertazzi*†,
Michele Goano*†, and Pierluigi Debernardi†
* Dipartimento di Elettronica e Telecomunicazioni, Politecnico di Torino, Corso Duca degli Abruzzi 24, 10129 Torino, Italy
† CNR-IEIIT, Corso Duca degli Abruzzi 24, 10129 Torino, Italy
E-mail: alberto.tibaldi@polito.it

***Abstract*—This paper presents the results of a physics-based time-domain simulator for a vertical-cavity surface-emitting laser (VCSEL). We implemented a trapezoidal rule second order backward differentiation formula (TR-BDF2) to simulate the large signal response of the device under investigation, including the parasitic effects of the pin junction arising from an interplay of optical and carrier transport phenomena.**

## I. Introduction

The last years witnessed growing attention toward the short and very-short haul optical communication, such as intra-datacenter or inter-chip optical links [1]. Targeting high-speed and minimal losses, vertical-cavity surface-emitting lasers (VCSELs) appear as the ideal choice. Indeed, VCSELs enable very high-speed operation thanks to their reduced active region volume. Direct modulation is possible, minimizing additional losses. Packaging and coupling with optical fibers are optimal, due to circular symmetry.

Usually, to simulate the VCSELs response, lumped parameters models are used [2], since they are simple, numerically fast and allow to obtain an analytical solution, which could be instrumental to interpret the device operation. However, this approach requires the introduction of many parameters, to be fitted with experimental data but generally not known when designing a novel structure. In this perspective, physics-based distributed models are more suitable for device-level design.

The starting point of this work is the 1-dimensional version of our in-house static physics-based solver [3], which couples a quantum-corrected drift-diffusion model to a photon rate equation containing some parameters extracted by an electromagnetic solver [4]. Regarding the dynamic response, the small signal analysis provides some useful information on the -3 dB VCSEL cutoff frequency, but in the case of a complex modulation scheme, *e.g.,* multi-level pulse amplitude modulation (PAM), a large signal analysis is necessary. For this reason, in this work we implemented a trapezoidal rule second order backward differentiation formula (TR-BDF2), which features the stability conditions suitable for the complex non-linear problem investigated here [5].

## II. Results and outlooks

The VCSEL under investigation consists of an $Al_xGa_{1-x}As$ oxide-confined 850 nm device formed of two distributed Bragg reflectors, which include 21 pairs for the top *p*-type mirror and 37 for the bottom *n*-type one. The active region embeds three 8 nm GaAs quantum wells (QWs). Additional details about the structure can be found in [6].

The solver is validated by comparing its output to an already implemented small signal solver and verifying that in steady state conditions its results are in agreement with the static solver.

Here, we present the results of a voltage step obtained by varying the injected current between 4 mA and 5.5 mA with a voltage rise time of 10 ps at T = 293 K. Let us define $I_n$ as the *n*-current at the *n*-contact, $I_{n,QW}$ as the total *n*-current entering into the QWs and $P$ as the optical output power. In Fig. 1, the aforementioned quantities are plotted as a function of time. Only the *n*-type current is plotted since the same behaviour holds for the *p*-type current. In the top plot we observe a very fast rise time of the current (black dots). The population that participates in the stimulated emission is however the one confined in the QWs. For this reason, the rise time of $I_{n,QW}$ (blue dots) is interpretable as the time that the carriers take to reach the active region, and therefore it represents an upper limit to the modulation speed. Such result highlights the power of the physics-based approach, as this delay is observable only by solving self-consistently the drift-diffusion, the quantum capture and the optical problem.

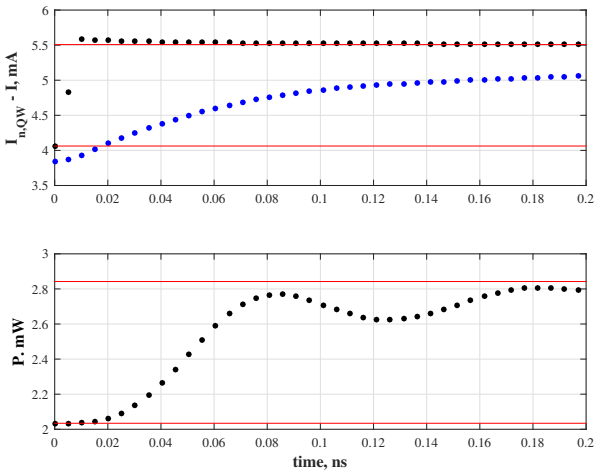


**Fig. 1:** top : QW (blue) and contact (black) currents. Bottom: output optical power. The red lines in the top plot are the high and low current regime values, while the red lines in the bottom plot are the high and low power regime values. The regime current injected into the QWs is slightly lower than the current at the contact due to leakage of carriers and bulk recombinations.

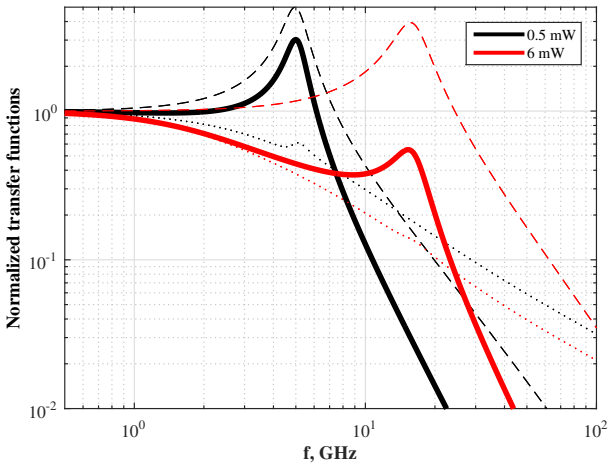


**Fig. 2:** normalized magnitude of the parasitic transfer function $H_p$ (dotted line), total transfer function $H_t$ (solid line) and ideal transfer function $H_i$ (dashed line) as defined in (1). In the total transfer function the amplitude goes down at -60 dB/dec, where -40 db/dec arise from the ideal laser second order response and -20 db/dec from the parasitic response. The -3dB cutoff frequency of the parasitic response is slightly decreasing for increasing optical power.

From a small signal perspective, a further understanding of the delay on the QWs current can be obtained by looking at the transfer functions. Let us define the total response $H_t(\omega)$, the parasitic response $H_p(\omega)$ and the ideal response $H_i(\omega)$:

$$H_t(\omega) = \frac{P(\omega)}{I(\omega)} = \frac{P(\omega)}{I_{QW}(\omega)} \frac{I_{QW}(\omega)}{I(\omega)} = H_i(\omega) H_p(\omega) \quad (1)$$

In Fig. 2 we plot the absolute values of the transfer functions, normalized to their value at $\omega = 0$. The transfer function between the current at the contact and the output power is the product between the ideal second order response of a laser and a parasitic response, which is a first-order low-pass response in agreement with the first-order time-domain evolution of the QW current (Fig. 1). In conclusion, this approach predicts in a natural way the junction parasitic delay and therefore can be used as a predictive tool for novel high speed structures.

The solver can be used to simulate complex modulation schemes and to obtain the eye diagrams. An external series resistance $R_s$ and parallel capacitance $C_p$ can be added and solved self-consistently to the system to account for extrinsic parasitics. Since in 1-dimensional solvers resistance is expressed in $\Omega\,\mathrm{m}^2$ and capacitance is expressed in $\mathrm{F/m}^2$, their product $\tau = RC$ is a time constant and can be chosen to fit experimental data. In Fig. 3, a 10 Gb/s eye diagram is obtained by plotting the optical power folded on two bit periods for a PAM modulation between 1 mA and 4 mA with a random sequence of 30 bits and $\tau = 50$ ps.

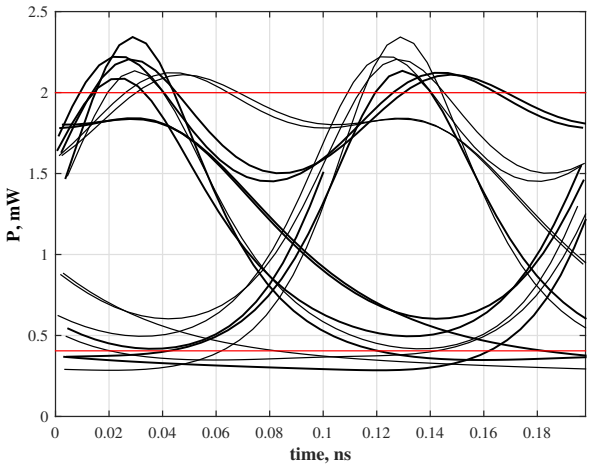


**Fig. 3:** example of 10 Gb/s eye diagram for a PAM modulation with a simulated sequence of 30 bits with $\tau = 50$ ps. The red lines are the high and low optical power regime values.

## III. Conclusions

Within a physics-based VCSEL simulation, only short sequences of bits can be simulated, due to its computational burden. Therefore, the natural continuation of this work is to identify a proper lumped model and its parameters to reproduce the results of the presented physics based analysis.

The simplest lumped model is a 2x2 system of equations [2], for photons and carriers. Since the time that carriers take to reach the active region is relevant, at least a third equation is needed [7]. The time-domain solver can be eventually used for a rigorous validation of the lumped model.

## References


[1] R. Baets, L. Vanwassenhove, "2D inter-chip optical interconnect" in Optical Materials, Volume 17, Issues 1–2, Pages 227-233, 2001, doi: https://doi.org/10.1016/S0925-3467(01)00047-7.

[2] Michalzik, R. (2013). "VCSEL Fundamentals". In: Michalzik, R. (eds) VCSELs. Springer Series in Optical Sciences, vol 166. Springer, Berlin, Heidelberg. https://doi.org/10.1007/978-3-642-24986-02

[3] A. Tibaldi, F. Bertazzi, M. Goano, R. Michalzik and P. Debernardi, "VENUS: A Vertical-Cavity Surface-Emitting Laser Electro-Opto-Thermal NUmerical Simulator," in IEEE Journal of Selected Topics in Quantum Electronics, vol. 25, no. 6, pp. 1-12, Nov.-Dec. 2019, Art no. 1500212, doi: 10.1109/JSTQE.2019.2893755.

[4] Gullino, A.; Tibaldi, A.; Bertazzi, F.; Goano, M.; Debernardi, P. "Reduced Dimensionality Multiphysics Model for Efficient VCSEL Optimization". Appl. Sci. 2021, 11, 6908. https://doi.org/10.3390/app11156908

[5] Dharmaraja, S. "An analysis of the TR-BDF2 integration scheme". http://hdl.handle.net/1721.1/41736

[6] P. Debernardi, A. Tibaldi, M. Daubenschüz, R. Michalzik, M. Goano and F. Bertazzi, "Probing Thermal Effects in VCSELs by Experiment-Driven Multiphysics Modeling," in IEEE Journal of Selected Topics in Quantum Electronics, vol. 25, no. 6, pp. 1-14, Nov.-Dec. 2019, Art no. 1700914, doi: 10.1109/JSTQE.2019.2927580.

[7] R. Nagarajan, M. Ishikawa, T. Fukushima, R. S. Geels and J. E. Bowers, "High speed quantum-well lasers and carrier transport effects," in IEEE Journal of Quantum Electronics, vol. 28, no. 10, pp. 1990-2008, Oct. 1992, doi: 10.1109/3.159508.